PULSATILE BLOOD FLOW IN THE ARTERIES

by

Gloria Adame Bennett

Thesis submitted to the Graduate Faculty of the

Virginia Polytechnic Institute and State University

in partial fulfillment of the requirements for the degree of

MASTER OF SCIENCE

in

Engineering Mechanics

APPROVED:

M. J. Werle, Chairman

J. E. Kaiser

J. Counts

D. Frederick

April, 1972

Blacksburg, Virginia

ACKNOWLEDGEMENTS

The author wishes to express her appreciation to her advisor of the Department of Aerospace Engineering and Applied Mechanics at the University of Cincinnati for his patience and encouragement throughout the course of this study.

The author is also grateful for the guidance and suggestions of other members of her committee.

The author wishes to express her appreciation to who typed this manuscript.

Finally, the author wishes to thank the Department of Engineering Mechanics for the funds used in the computer analysis and the National Defense Education Act for the fellowship that made this thesis possible.

TABLE OF CONTENTS

LIST OF SYMBOLS

$A(z)$	boundary condition on vorticity at the vessel wall
b	arbitrary constant used to adjust the extent of the transition region
c	wave speed
c_o, c_p, c_1	wave speed at the particular subscripted cross section
f	nondimensional stream function
F	parameter describing flow situation, contains outflow
g	nondimensional vorticity
m	arbitrary constant used to adjust the extent of the transition region
n	nondimensional radial coordinate
p	local pressure
p_m	local mean pressure
p_o	reference pressure
q_o	volume rate of flow at the reference cross section
r	radial coordinate
R	local radius
R_m	local mean radius
R_o	radius at the reference cross section
RE	Reynolds number
S	local cross sectional area
t	time
T	nondimensional time
u	fluid velocity in the axial direction
U_m	mean fluid velocity

v	fluid velocity in the radial direction
v_r	radial fluid velocity due to change in radius with respect to time
v_s	radial fluid velocity due to outflow
w	vorticity
x	axial coordinate, distance from heart
z	nondimensional axial coordinate
$\alpha_1, \alpha_2, \alpha_3$	coefficients of a differential equation
β	arbitrary constant
$\beta_1, \beta_2, \beta_3$	coefficients of a differential equation
$\gamma_1, \gamma_2, \gamma_3$	coefficients of a differential equation
ρ	fluid density
Δ	incremental step change
∇^2	Laplacian operator
θ	tangent to vessel at the proximal end of the transition region
Ψ	stream function
μ	fluid viscosity

LIST OF ILLUSTRATIONS

I. INTRODUCTION

A. History of Blood Flow Analysis

Prior to the nineteenth century the models developed to represent the human cardiovascular system were primarily descriptive in nature. The Harvey model, developed circa 1600, was the first correct physiological description of the circulation. Over the next three hundred years only incremental changes were made to improve description of the pulmonary and capillary systems. A theoretical model for the cardiovascular system began to emerge during the nineteenth century. In 1840 Poiseuille conducted experiments on viscous fluids flowing in rigid tubes which later led to the Hagen-Poiseuille equation used today. In 1755 Euler postulated the governing equations for fluid flow in a flexible tube which were not solved in the blood flow context until 1956. Then in 1958 Womersley published a wave propagation model for blood flow in arteries of constant cross section which reasonably predicted flow quantities in short vascular segments [1].*

In the late 1960's Anliker, Rockwell and Ogden [2] developed a one-dimensional, nonlinear analysis of large amplitude waves propagating in tapering elastic arteries. Their nonlinear analysis simulated the experimentally observed phenomena by predicting the pronounced steepening of wave fronts and peaking of pulses which propagate down the arterial tree. Their study also indicated that nonlinear effects must be accounted for in order to correctly interpret small changes in

---

*Numbers in brackets correspond to references in Bibliography.

the flow and pressure pulses. Anliker's success in predicting changes in the pulses may be partly attributed to his direct incorporation of vessel wall properties in the wave speed expression.

Anliker's model also proposed relationships for local changes in cross sectional area, friction expressions and outflow expressions for regions above and below the femoral artery. Each expression was based on experimental data from various other authors and then scaled down or up to fit a standard case. The friction expressions are questionable because of the assumption of quasi-steady flow and the outflow expressions are questionable because they prescribe steady, continuous leakage across the vessel wall in place of outflow at discrete locations along the artery. The empirical expressions in Anliker's model contain room for improvement since the assumptions are gross approximations of the real situation.

B. Current Approaches

The arterial side of the cardiovascular system may be divided into three fluid flow regimes as follows: a) the arteries which are best described by viscous unsteady flow, b) the arterioles which may possibly be described by rheolgical models, c) the capillaries which are best described by plug flow. Arterial blood flow studies may be further categorized into three groups which are: a) linearized, two-dimensional governing equations whose solutions are periodic, b) nonlinear, one-dimensional governing equations, c) analog computer models [3].

Womersley made extensive contributions to the model based on two-dimensional, linearized governing equations. The blood was assumed to

be Newtonian and incompressible, flowing in axisymmetric, laminar fashion. The vessel was modeled as cylindrical, infinitely long and under a steady pressure. Womersley arrived at closed form solutions in terms of Bessel functions periodic in time. His model predicts that waves damp out as they propagate down the vessel which does not agree with observed phenomena. However, the model predicts instantaneous flow velocities based on the pressure gradient at a point in the flow field [4].

The second category of blood flow models is based on the one-dimensional, nonlinear governing equations. Assumptions used for the blood and the vessel remain unchanged. This model has proven amenable for study of leakage effects, entrance effects, variations in shear or viscosity of the blood and the study of pulsatile flow development. The governing equations are solved numerically using the method of characteristics where the flow situation is constructed by tracing one wavelet as it propagates in the time and space planes. This model predicts that wave velocity decreases with increasing pressure which contradicts experimental observations. Nevertheless, the model does predict flow quantities over short segments of the arterial tree [3].

Analog computer solutions to blood flow models generally use the one-dimensional equations. Use of the analog computer facilitates input of recorded pressure gradients and allows the blood viscosity to change such that it remains proportional to the average velocity. Analog solutions compare favorably with Womersley's modified model for wave reflections. The analog model produces relations for changes in instantaneous pressure and velocity and yields flow and pressure

waveforms similar to those observed experimentally [3].

Mathematical modeling of the cardiovascular system has been done only for the arterial side. Difficulties involved in modeling the venous system include the elliptical shape of the veins, their tendency to collapse intermittently, and the unsteady nature of the blood flow driven by the skeletal muscles and abdominal muscle pump. Modeling of the arterial system has been limited to the artery and capillary levels. The arterioles, which contribute the largest portion of resistance in the system and damp out the pulsations caused by the heart [5], have been almost entirely neglected. The behavior of the blood is markedly non-Newtonian at this level and thus far best described as a Bingham plastic [6]. Description of leakage from the arterial tree has been limited to continuous functions while in reality the leakage occurs at discrete locations over regular intervals.

Review of the literature illustrates a need for a blood flow model based on the two-dimensional, nonlinear, unsteady governing equations. The solutions would provide a standard for comparing the linearized and the one-dimensional models presently appearing in the literature.

C. Approach and Goal

In the past, the cardiovascular system was studied in order to increase understanding of the physiological processes taking place. Increased understanding led to improved treatments and new diagnostic techniques. The fluid mechanical behavior of the cardiovascular system is being studied to better understand "the control mechanisms

responsible for maintaining and regulating blood flow" [2]. The physiology and fluid mechanics are coupled such that changes in the fluid mechanical variables or parameters could be used as diagnostic indicators of changing health. In recent years, the development of more capable digital computers and non-invasive flow and pressure measurement devices is making it possible to study the human circulation under almost natural conditions without the anesthetics or trauma related to surgery. Further improvements are necessary in both instrumentation and mathematical modeling of the cardiovascular system before the models can be used as reliable diagnostic tools.

The present study is a direct extension of Anliker's work to two space variables. A blood flow model is derived based on the unsteady, axisymmetric, nonlinear partial differential equations for pulsatile flow in a flexible tube. The working fluid, blood, is assumed to be viscous, incompressible and homogeneous flowing in laminar fashion. The vessel is assumed circular in cross section and tapering with increasing distance from the heart.

The purpose of this study is to solve a simplified version of the governing equations in order to demonstrate an approach to solving the equations for a general blood flow situation. The simplified version is solved numerically using the central finite difference form of the governing equations and the Alternating Direction-Implicit method.

The results obtained from this study stem from two sources: a) test case programs of only the stream function equation or the vorticity equation, b) a combined program in which both the stream

function and the vorticity equations are integrated. The first category of results is from cases in which the initial conditions for both the stream function and the vorticity are zero and Poiseuille flow is imposed at the proximal end of the vessel. Results from both sources show that the stream function and vorticity converge to the exact solution so that the effect of the initial conditions is damped out and does not alter the steady state solution. The second category of results is from cases in which the initial conditions are chosen indentical to the anticipated steady state solution and pulsating Poiseuille flow is introduced into the nonlinear coefficients of the vorticity equation. The results demonstrate the effect of the pulsating input only in the vorticity solution.

II. GOVERNING EQUATIONS

A. Physical Model

Information and auxiliary relations must be introduced to justify the assumptions made in deriving a mathematical model for the cardiovascular system. Human blood is a suspension of red blood cells, white blood cells, platelets, hormones, ions, nutrients and proteins in a fluid plasma. The blood is chemically about eighty percent water [7] which allows the assumption of incompressibility to be valid. A healthy human being has a hemotocrit of forty-five percent [5], meaning that blood cells occupy forty-five percent of his total blood volume. Such a large percentage of particles in suspension affects the behavior of the fluid. However, at the arterial level the ratio of characteristic dimensions of the blood vessel diameter to a red blood cell is about three thousand to one (3,000:1). This ratio is large enough to permit the blood to be considered homogeneous and allow the assumption that it behaves as a Newtonian fluid with an apparent viscosity several times higher than the viscosity of the plasma alone. Womersley and Anliker have verified these assumptions by favorable comparison of their models with experimental data.

The arteries are distensible elastic vessels that taper geometrically and change their elastic properties with increasing distance from the heart. The vessels are constrained longitudinally but upon chemical or nervous stimulus become free to expand radially to accommodate changes in relative volume up to four times normal capacity [8].

The model proposed by Anliker assumes the blood to be viscous and incompressible and the vessel as a circular, tapering elastic tube. Viscosity effects are modeled by algebraic friction expressions for laminar or turbulent flow but are restricted by the assumption of quasi-steady flow. Branching of the arteries and the consequent leakage, or mean normal outflow at each discrete branch, is modeled by continuous, distributed functions above and below the femoral artery. Any local area changes are expressed as exponential functions depending on pressure and distance from the heart.

Anliker's approach to quantifying the physical properties of the vessel is new in that the properties are introduced directly through the wave speed. The information that wave speed is a linear function with respect to pressure is attributed to M. B. Histrand [2] and that it is a linear function with respect to distance from the heart is attributed to D. A. McDonald [2]. The wave speed expression is then given by [2]

$$c = (c_0 + c_1 p)(1 + nx) \quad . \qquad 2.1$$

Since Anliker's model is one-dimensional, the pressure in Equation 2.1 is a spatial average pressure at a particular cross section. Thus, in a two-dimensional analysis the pressure in the wave speed expression is modified to be the mean pressure given by

$$p_m = \frac{2\int_0^R p r\, dr}{R^2} \quad . \qquad 2.2$$

The blood vessel is free to expand and contract radially upon stimulus. The axial range of an expansion or contraction in a vessel is termed the transition region and is illustrated in Figure 1. Because of the change in cross sectional area across the transition region and the necessity of maintaining a particular volume flow rate, the pressure and wave speed must also undergo related changes across the transition region. For slight changes in area over long distances, the wave speed changes only perceptibly. But large changes in area over short distances cause the wave speed to change considerably. Proper incorporation of an exponential function into Equation 2.1 yields the changes experienced over a transition region and is given as

$$c = \frac{(c_0 + c_1 p)(1 + nx)}{1 - \ell^{-(x+b)^m}} , \qquad 2.3$$

where b and m are arbitrary constants used to adjust the extent of the transition region.

Anliker developed two relations for wave speed; one was Equation 2.1 which arose from experimental observations and the other came from his analysis by the method of characteristics given as [2]

$$c = \sqrt{\frac{S}{\rho\left(\frac{\partial S}{\partial p}\right)_z}} . \qquad 2.4$$

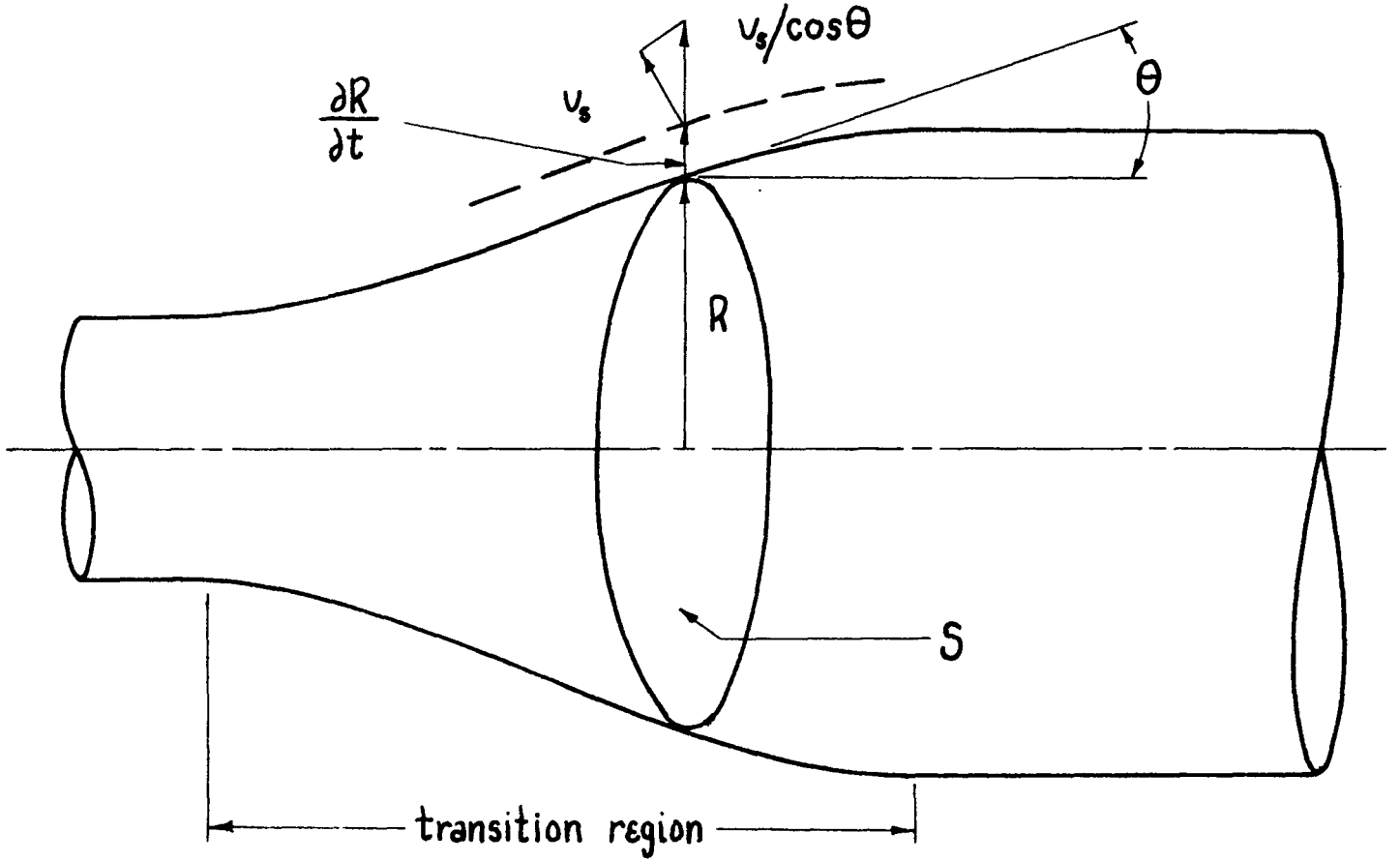

Figure 1. Illustration of distensible vessel and related quantities

He combined Equations 2.1 and 2.4, then integrated the resulting differential equation to produce an equation for the local changes in cross sectional area in terms of pressure, wave speed and distance from the heart. The equation is [2]

$$S = \pi R^2 = \pi R_o^2 \, e^{\left[-\beta x + \frac{p - p_o}{\rho c_p c_o}\right]}, \qquad 2.5$$

where p_o and R_o are constants at $x = 0$. Figure 1 illustrates the quantities used in Equation 2.5.

B. Mathematical Model

The mathematical model is derived on the basis of the relations just introduced for the behavior of the blood and for the geometric changes occuring in the blood vessel. Fluid flow is considered axisymmetric, laminar and periodic in time with the blood modeled as a Newtonian, incompressible fluid. The blood vessel is assumed to be a distensible, circular cylinder tapering with increasing distance from the heart. Figure 2 illustrates a schematic of the blood vessel with the coordinate system and related quantities used in deriving the governing equations.

Expressed in cylindrical coordinates, the continuity equation is

$$\frac{\partial u}{\partial x} + \frac{\partial v}{\partial r} + \frac{v}{r} = 0 , \qquad 2.6$$

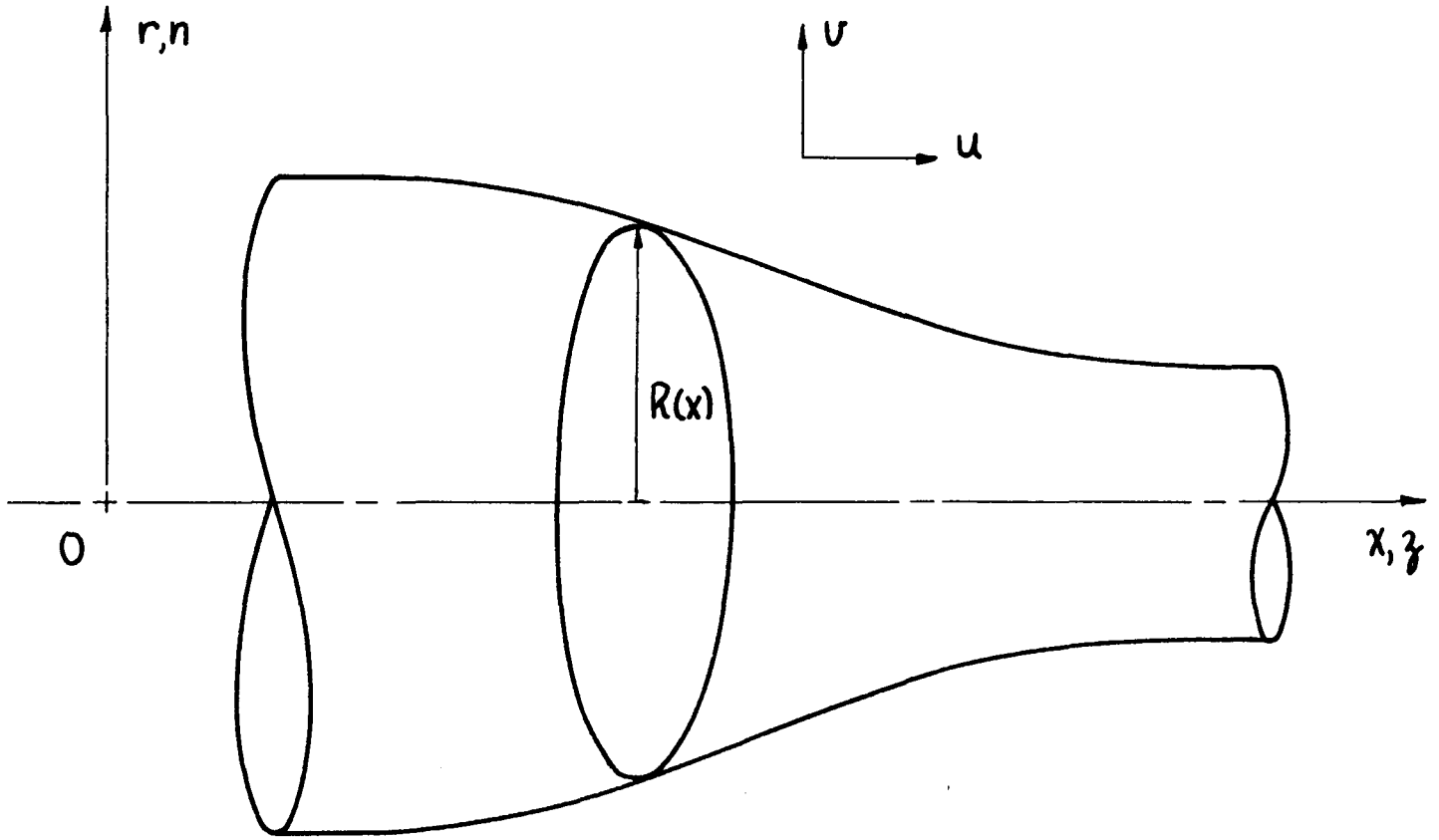

Figure 2. Illustration of coordinate systems and variables

and the momentum equations are

$$\frac{\partial u}{\partial t} + u\frac{\partial u}{\partial x} + v\frac{\partial u}{\partial r} + \frac{1}{\rho}\frac{\partial p}{\partial x} = \nu\left[\frac{\partial^2 u}{\partial r^2} + \frac{1}{r}\frac{\partial u}{\partial r} + \frac{\partial^2 u}{\partial x^2}\right], \qquad 2.7$$

and

$$\frac{\partial v}{\partial t} + u\frac{\partial v}{\partial x} + v\frac{\partial v}{\partial r} + \frac{1}{\rho}\frac{\partial p}{\partial r} = \nu\left[\frac{\partial^2 v}{\partial r^2} + \frac{1}{r}\frac{\partial v}{\partial r} + \frac{\partial^2 v}{\partial x^2} - \frac{v}{r^2}\right]. \qquad 2.8$$

Boundary conditions for the flow situation depicted in Figure 1 and 2 are the following:

a) at the center of the vessel where r = 0,

$$\left(\frac{\partial u}{\partial r}\right) = 0$$
$$v = 0 \qquad 2.9$$
$$\left(\frac{\partial p}{\partial r}\right) = 0$$

b) at the vessel wall where r = R,

$$u = 0$$
$$v = \frac{\partial R}{\partial t} + \frac{v_s}{\cos\theta} \qquad 2.10$$
$$\theta = \tan^{-1}\left(\frac{\partial R}{\partial x}\right)$$

c) at the proximal end of the vessel where x = 0,

$$u = \frac{q_o}{\pi R_o^2}$$
$$v = 0 \qquad 2.11$$
$$p = \text{unknown}$$

where q_o is periodic in time,

d) at the distal end of the vessel where x = L,

$$\frac{\partial}{\partial t} = 0$$

$$p = \text{constant} \quad . \tag{2.12}$$

The problem as posed thus far involves two strongly coupled, second order, nonlinear partial differential equations. Conditions at the boundaries are somewhat less than ideal since: a) pressure is unknown at the proximal end, b) radial fluid velocity at the wall depends on elastic wall properties and on wall displacement changes with respect to time, c) the inside radius of the vessel is not known precisely because of the changes in the thickness of the wall as the vessel expands and contracts.

In order to simplify analysis of the problem it is reformulated in terms of the stream function and vorticity. The stream function is defined by

$$u = \frac{1}{r} \frac{\partial \psi}{\partial r} \tag{2.13}$$

$$v = \frac{-1}{r} \frac{\partial \psi}{\partial x} \quad , \tag{2.14}$$

and the vorticity is given as

$$w = \frac{\partial v}{\partial x} - \frac{\partial u}{\partial r} \quad . \tag{2.15}$$

These substitutions for the components of velocity completely satisfy the continuity equation leaving the momentum equations in terms of vorticity and the stream function unsolved. The system of governing equations is reduced to

$$\nabla^2 \Psi = -\omega r, \tag{2.16}$$

and

$$r\frac{\partial \omega}{\partial t} + \frac{\partial \Psi}{\partial r}\cdot\frac{\partial \omega}{\partial x} - \frac{\partial \Psi}{\partial x}\cdot\frac{\partial \omega}{\partial r} + \frac{\omega}{r}\cdot\frac{\partial \Psi}{\partial x} = \frac{\partial}{\partial r}\left[\frac{\partial^2 \omega}{\partial r^2} + \frac{1}{r}\cdot\frac{\partial \omega}{\partial r} - \frac{\omega}{r^2} + \frac{\partial^2 \omega}{\partial x^2}\right]. \tag{2.17}$$

Boundary conditions on this system are the following:

a) at r = 0,

$$\Psi = 0$$
$$\omega = 0 \tag{2.18}$$

b) at r = R,

$$\left(\frac{\partial \Psi}{\partial r}\right) = 0$$
$$\Psi = \frac{q_0}{2\pi} - \int_0^x R v\, dx \tag{2.19}$$
$$v = \frac{\partial R}{\partial t} + \frac{v_s}{\cos\theta}$$

c) at x = 0,

$$\Psi = \frac{r^2 q_0}{2\pi R_0^2}$$
$$\omega = 0 \tag{2.20}$$

d) at x = L,

$$v_s = 0$$
$$v_r = 0 \tag{2.21}$$

Noting the conditions imposed on the radial velocity component, Equation 2.14 leads to the condition that

$$\left(\frac{\partial \Psi}{\partial X}\right)_{L,R} = 0. \qquad 2.22$$

Consequently, flow near the distal end of the vessel approaches Poiseuille flow. If the radius is allowed to become a constant function of the axial coordinate beyond the point $x = L$, Poiseuille flow occurs a short distance away at $x = L + L_2$. Allowing $L_2 = 0$ and placing the Poiseuille solution at $x = L$ requires use of the condition that

$$\left(\frac{\partial \omega}{\partial X}\right)_{L,R} = 0. \qquad 2.23$$

Figure 3 illustrates the location of quantities used to specialize boundary conditions in the vessel.

The last major step in deriving the governing equations involves redefining the coordinates, the stream function and the vorticity in terms of non-dimensional quantities. The transformed variables are

$$\eta = \frac{r}{R} \qquad f = \frac{\Psi}{F}$$

$$z = \frac{x}{R} \qquad 2.24$$

$$\tau = \frac{t U_m}{R_m} \qquad g = \frac{-R^3}{F}\omega \,,$$

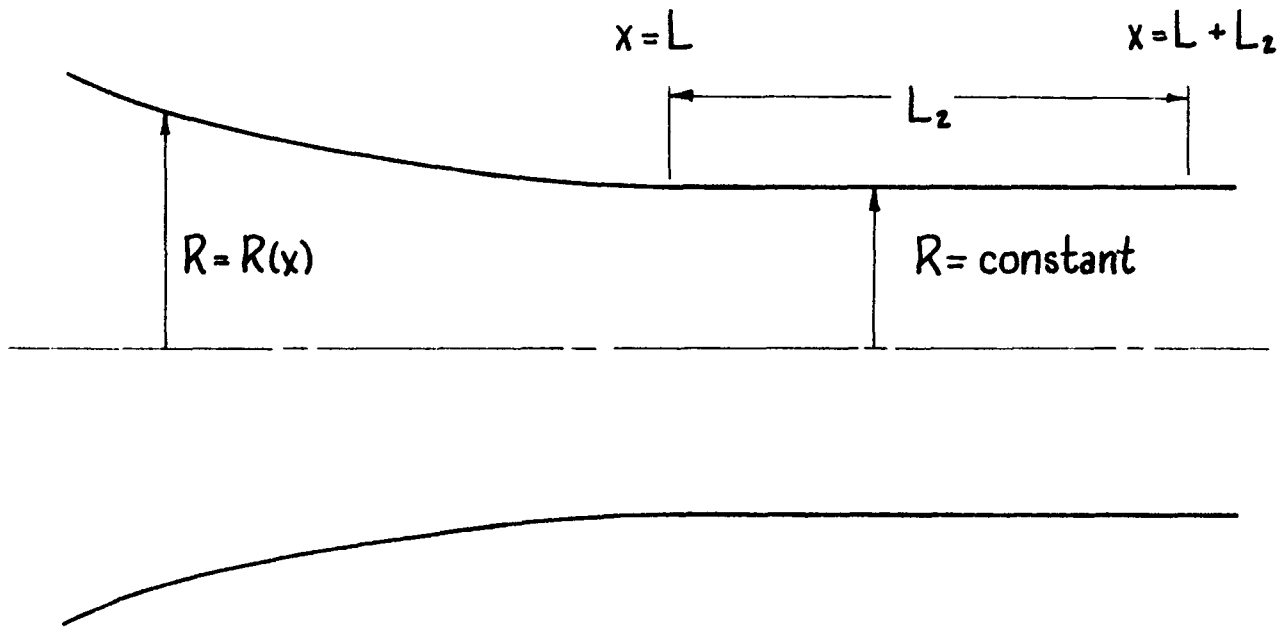

Figure 3. Distal end of vessel

where U_m and R_m are the mean velocity and mean radius. The dimensionless vorticity is g and the dimensionless stream function is f, with R being the local radius of the vessel and F a parameter depending on the nature of the flow. The dimensionless coordinates are n, z and T. These substitutions into the governing equations result in considerable expansion containing terms that allow for changes in wave speed, vessel diameter and local outflow. The purpose in deriving the transformed equations is to funnel these changes into the nonlinear coefficients of the governing equations. As a result, this leaves the boundary conditions normalized to constants. The transformed equation for the stream function is

$$\left[1+n^2R_x^2\right]f_{nn} + \left[\frac{-1}{n} + n\left\{2R_x(zR_x-1)\frac{F_z}{F} + 2R_x^2 - RR_{xx}\right\}\right]f_n + \left[(1-zR_x)^2\frac{F_{zz}}{F} + (2zR_x^2 - zRR_{xx} - 2R_x)\frac{F_z}{F}\right]f - \left[2nR_x(1-zR_x)\right]f_{nz} + \left[2(1+zR_x)^2\frac{F_z}{F} + 2zR_x^2 - zRR_{xx} - 2R_x\right]f_z + \left[1-zR_x\right]^2 f_{zz} = ng. \qquad 2.25$$

The transformed equation for vorticity is

$$g_{nn} + \left[\frac{1}{n} + 8nR_x^2 - nRR_{xx} - nRR_x\frac{F_z}{F} + nRR_TRE\right.$$

$$+\frac{F}{R}RER_xf_n + \frac{F}{R}\frac{RE}{n}\left\{(1-zR_x)f_z + (1-zR_x)\frac{F_z}{F}f\right.$$

$$\left.\left. - nR_xf_n\right\}\right]g_n - \left[\frac{1}{n^2} + 6R_x(1-zR_x)\frac{F_z}{F} + 3RR_{xx}\right.$$

$$-12R_x^2 - (2zR_x^2 - zRR_{xx} - 2R_x)\frac{F_z}{F} - R(1-zR_x)\frac{F_{zz}}{F}$$

$$\frac{-F}{R}\frac{RE}{n}\left\{3n\frac{R_T}{F} + nz\frac{R^2}{F^2}F_z - n\frac{R^3}{F^2}F_T + 3R_xf_n\right.$$

$$-(1-zR_x)\frac{F_z}{F}f_n - (1-zR_x)\frac{f_z}{n} - (1-zR_x)\frac{F_z}{F}\frac{f}{n}$$

$$\left.+R_xf_n\right\}\Big]g + \left[RRE\right]g_T - \left[nRR_x\right]g_{nz} + \left[2zR_x^2\right.$$

$$-zRR_{xx} - 2R_x + R(1-zR_x)\frac{F_z}{F} - 6R_x(1-zR_x) + zRR_TRE$$

$$\left.\frac{-F}{R}\frac{RE}{n}(1-zR_x)f_n\right]g_z + \left[R(1-zR_x)\right]g_{zz} = 0. \qquad 2.26$$

The boundary conditions for this system of equations are:

a) at $n = 0$,

$$f(z,0) = 0 \tag{2.27}$$

$$g(z,0) = 0 \tag{2.28}$$

b) at $n = 1$,

$$f(z,1) = 1 \tag{2.29}$$

$$\left(\frac{\partial f}{\partial n}\right)_{z,1} = 0 \tag{2.30}$$

c) at $z = 0$,

$$f(0,n) = 2n^2 - n^4 \tag{2.31}$$

$$g(0,n) = -8n$$

d) at $z = 1$,

$$\left(\frac{\partial f}{\partial z}\right)_{1,n} = 0 \tag{2.32}$$

$$\left(\frac{\partial g}{\partial z}\right)_{1,n} = 0$$

Derivation of the mathematical model including both the nonlinear and two-dimensional characteristics of blood flowing in a distensible vessel is complete. It is emphasized that numerical results obtained from this study do not include the many details contributed by other authors but merely show that meaningful results are obtainable from a more generalized model than is currently appearing in the literature.

C. Simplified Model

Poiseuille flow in a rigid tube is a simplified version of the governing equations derived thus far. The techniques used in solving the system of governing differential equations is tested on this simple application since the numerics should not be much worse for

the general case in which all the secondary changes appear only in the nonlinear coefficients. For Poiseuille flow, the radius R is a constant in time and space and the parameter F is a constant for steady flow or contains a cosine function in the unsteady case. The simplified steady state version of the vorticity equation is

$$g_{nn} + \left[\frac{1}{n} + \frac{RE}{n} f_z\right] g_n - \left[\frac{1}{n^2} + \frac{RE}{n^2} f_z\right] g$$

$$+ \left[g_{zz} - \frac{RE}{n} f_n g_z - RE g_r\right] = 0 , \qquad 2.33$$

and the stream function is reduced to

$$f_{nn} - \frac{1}{n} f_n + f_{zz} = ng . \qquad 2.34$$

Equation 2.34 can be made artificially parabolic by introducing a derivative with respect to time as

$$f_{nn} - \frac{1}{n} f_n + f_{zz} - f_r = ng. \qquad 2.35$$

The derivative with respect to time is used as a relaxation parameter since as time increases, the derivative tends toward zero. This derivative with respect to time has no relation to real time but is merely used as an iteration tool in the numerical solution.

The solutions for Poiseuille flow are

$$f = 2\eta^2 - \eta^4 \ , \qquad 2.36$$

and

$$g = -8\eta \ . \qquad 2.37$$

The Alternating Direction-Implicit numerical method is applied to the simplified form of the governing equations.

III. NUMERICAL SOLUTION

A. Choice of Numerical Method

The governing partial differential equations for blood flow in large arteries, Equations 2.25 and 2.26, are written in terms of the dimensionless stream function and the dimensionless vorticity. The differential equation for vorticity is parabolic with respect to time and elliptic with respect to space while the differential equation for the stream function is elliptic with respect to space. A choice between the explicit and implicit numerical methods depends upon the form in which the time dependent term is written in the finite difference equation. For this study the implicit method is used since convergence and stability of the solution is insured [9]. In addition, the implicit method allows greater freedom in the choice of time and spatial step sizes but requires more complex calculations at each time step.

Consider the general form of a simple parabolic differential equation written explicitly in one direction as

$$\frac{\partial^2 F}{\partial \eta^2} + \gamma_1 \frac{\partial F}{\partial \eta} + \gamma_2 F + \gamma_3 - \frac{\partial F}{\partial T} = 0 . \qquad 3.1$$

The central finite difference form of Equation 3.1 is

$$\frac{F_{j+1}^{K+1} - 2F_j^{K+1} + F_{j-1}^{K+1}}{(\Delta\eta)^2} + \gamma_1 \frac{F_{j+1}^{K+1} - F_{j-1}^{K+1}}{2\Delta\eta} +$$

$$\gamma_2 F_j^{K+1} + \gamma_3 - \frac{F_j^{K+1} - F_j^K}{\Delta T} = 0 , \qquad 3.2$$

where the j subscript refers to spatial increments in the n direction and the k superscript refers to time increments. Collecting terms with like j subscripts and like k supercripts gives

$$\left[\frac{1}{(\Delta n)^2} - \frac{\gamma_1}{2\Delta n}\right] F_{j-1}^{K+1} + \left[\gamma_2 - \frac{2}{(\Delta n)^2} - \frac{1}{\Delta T}\right] F_j^{K+1}$$

$$+\left[\frac{1}{(\Delta n)^2} + \frac{\gamma_1}{2\Delta n}\right] F_{j+1}^{K+1} = -\gamma_3 - \frac{F_j^K}{\Delta T} . \qquad 3.3$$

In this manner a single differential equation is shown to contain the solution at the forward (k + 1) time step and yields equation of the form

$$AF_{j-1}^{K+1} + BF_j^{K+1} + CF_{j+1}^{K+1} = CD_j^K . \qquad 3.4$$

Given the grid of points M x M as shown in Figure 4, the left hand side of Equation 3.4 is limited to three stations at the forward time step while the right hand side is a known value from the previous time step. Writing out Equation 3.4 at each station results in a set of M-2 linear algebraic equations during each time step. These

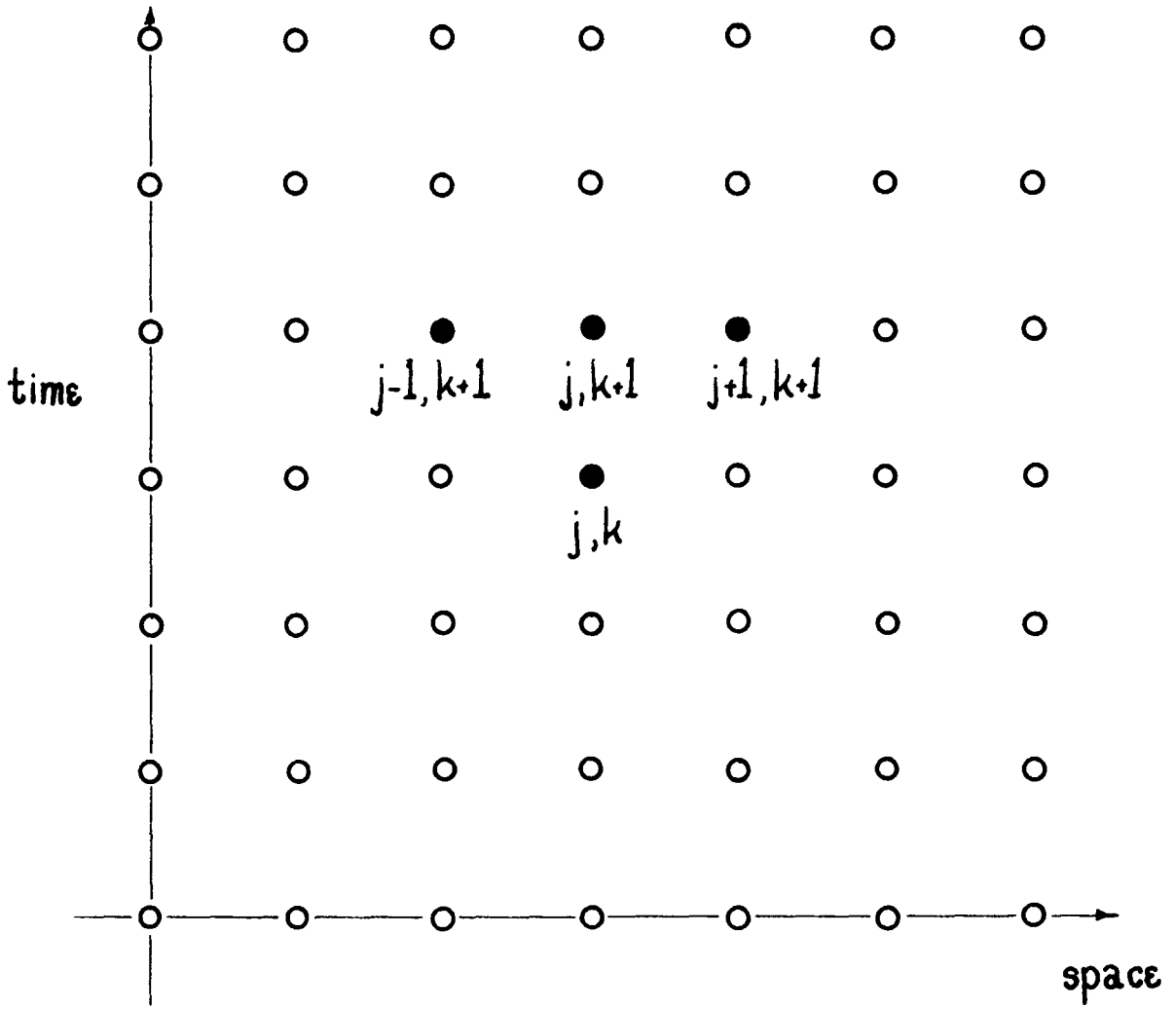

Figure 4. Illustration of grid MxM

equations form a tridiagonal matrix of coefficients whose terms appear only above the main diagonal. Each boundary point on the grid is defined by the boundary conditions leaving a system of M-2 equations and M-2 unknowns to be solved at each time step.

B. Alternating Direction-Implicit Method

The governing partial differential equations for vorticity and the stream function are parabolic with respect to time or may be made artificially parabolic for relaxation purposes. Both Equations 2.33 and 2.34 contain derivatives with respect to the axial and the radial coordinates. Numerical solution of this set of equations is accomplished by operation on each separate equation with the Alternating Direction-Implicit (ADI) method.

The ADI method uses a differential equation twice during any full time step. The general form of a parabolic partial differential equation is

$$\gamma_1 \frac{\partial^2 F}{\partial r^2} + \gamma_2 \frac{\partial^2 F}{\partial z^2} + \gamma_3 \frac{\partial F}{\partial r} + \gamma_4 \frac{\partial F}{\partial z} + \gamma_5 \frac{\partial F}{\partial T} + \gamma_6 F + \gamma_7 = 0. \qquad 3.5$$

Since the ADI method is designed to integrate in one direction at a time, Equation 3.5 must be rewritten for the first one-half time step as

$$\frac{\partial^2 F}{\partial r^2} + \alpha_1 \frac{\partial F}{\partial r} + \alpha_2 F + \alpha_3 - \frac{\partial F}{\partial T} = 0, \qquad 3.6$$

and for the second one-half time step as

$$\frac{\partial^2 F}{\partial \bar{z}^2} + \beta_1 \frac{\partial F}{\partial \bar{z}} + \beta_2 F + \beta_3 - \frac{\partial F}{\partial T} = 0. \qquad 3.7$$

For the first one-half time step the difference equation is written in the normal direction by combining derivatives with respect to the axial coordinate and time in the f term and remainder term. Writing out Equation 3.6 in finite difference form and combining like j subscripted terms and like k superscripted terms results in an equation of the form

$$AF_{j-1}^{K+1} + BF_{j}^{K+1} + CF_{j+1}^{K+1} = CD_{j}^{K} \quad , \qquad 3.8$$

as previously discussed in Equation 3.4. The coefficients of Equation 3.8 are given by Equation 3.3. These coefficients are computed at each station and form the tridiagonal matrix mentioned earlier. The solution of this set of linear algebraic equations is valid at the one-half time step. This solution is then used as an input for the second one-half time step in which the differential equation is written in the axial direction. Coefficients of Equation 3.8 are again computed at each station resulting in a second tridiagonal matrix. The solution of the second set of linear algebraic equations is valid at the full time step. In this manner, each of the two-dimensional parabolic governing differential equations is integrated in one direction during the first one-half time step, then

integrated in the other direction during the second one-half time step.

The difference equations used in the computer programs are written in the central difference form for the first and second partial derivatives with respect to space and in the implicit form for the derivative with respect to time as follows:

$$\frac{\partial F}{\partial z} = \frac{F_{i+1,j} - F_{i-1,j}}{2\Delta z} ,$$

$$\frac{\partial^2 F}{\partial z^2} = \frac{F_{i+1,j} - 2F_{i,j} + F_{i-1,j}}{(\Delta z)^2} , \qquad 3.9$$

$$\frac{\partial F}{\partial n} = \frac{F_{i,j+1} - F_{i,j-1}}{2\Delta n} ,$$

$$\frac{\partial^2 F}{\partial n^2} = \frac{F_{i,j+1} - 2F_{i,j} + F_{i,j-1}}{(\Delta n)^2} ,$$

$$\frac{\partial F}{\partial T} = \frac{F^{k+1} - F^{k}}{\Delta T} .$$

The i subscript refers to spatial increments in the z direction, the j subscript refers to spatial increments in the n direction and the k superscript refers to increments in time. Since the present study involves solving two coupled, second order partial differential

equations, the ADI method is used on each one separately in such a manner that the set of governing equations is solved iteratively.

C. Numerical Scheme

The computer program was written in Fortran IV language for use on the IBM 360 computer. A general outline of the steps used in solving the governing equations is the following. The equation for vorticity, Equation 2.33, is first integrated in the normal direction during a real one-half time step and then the stream function, Equation 2.35, is integrated in both directions. Since Equation 2.35 is artificially parabolic, the time term is used as a relaxation parameter. The program iterates on the stream function integrations in order to satisfy the boundary condition at the wall given in Equation 2.29. The vorticity equation is then integrated in the axial direction during a second real one-half time step and the program iterates on the stream function integrations once again. Time is incremented and the entire process is repeated for the next time step.

A flow chart of the entire numerical scheme is shown in Figure 5. In greater detail, the program operates in sections of which the bookkeeping portion first reads in data, defines constants and step sizes and sets up the grid used in the numerical calculations. Next, the stream function and vorticity matrices are initialized to some known condition. Since the vorticity depends on changes in the stream function the problem solution is carried out with the following scheme.

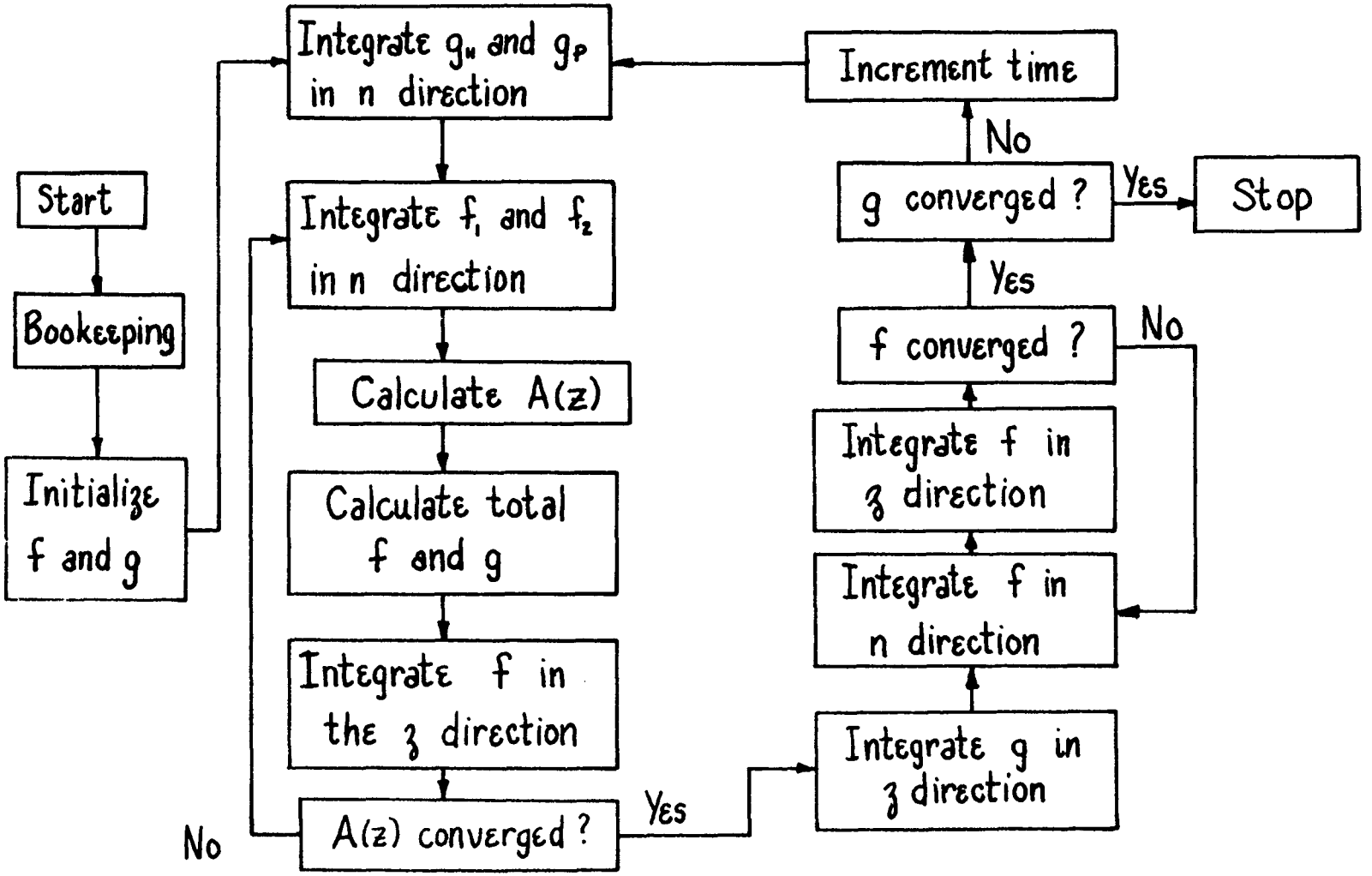

Figure 5. Flow chart illustrating numerical scheme

Recall that the boundary conditions at the wall, Equations 2.29 and 2.30, completely define the stream function but leave the vorticity unspecified. The boundary condition at the wall for the vorticity is defined by separating the vorticity into two parts. This separation can be accomplished because Equation 2.33 is a linearized form of the general case. The vorticity is separated into a homogeneous and a particular part and then integrated in the normal direction using the following equations and boundary conditions. Let

$$g = A g_{Homogeneous} + g_{Particular} \,, \tag{3.10}$$

where A is a constant at each station. Then the homogeneous part of the vorticity is g_H which satisfies the equation

$$\frac{\partial^2 g_H}{\partial n^2} + \alpha_1 \frac{\partial g_H}{\partial n} + \alpha_2 g_H = 0 \,, \tag{3.11}$$

where

$$g_H(0) = 0 \,, \tag{3.12}$$

$$g_H(1) = 1 \,, \tag{3.13}$$

and the particular part is g_P which satisfies

$$\frac{\partial^2 g_P}{\partial n^2} + \alpha_1 \frac{\partial g_P}{\partial n} + \alpha_2 g_P + \alpha_3 = 0 \,, \tag{3.14}$$

where

$$g_P(0) = 0 \,, \tag{3.15}$$

$$g_P(1) = 0. \tag{3.16}$$

The condition along the axis is completely satisfied by Equations 3.12 and 3.15 while the condition at the wall becomes

$$g(1) = A \quad , \tag{3.17}$$

from Equations 3.13 and 3.16. The numerical solution of the homogeneous and particular parts of the vorticity are used as inputs to the stream function integrations.

The stream function, Equation 2.34, is also a linear form of the general case and can be separated into two particular parts and integrated in the normal direction using the following equations and boundary conditions. Let

$$f = Af_1 + f_2 \quad , \tag{3.18}$$

where A is the same constant used in Equation 3.10. Then the first particular part of the stream function is f_1 which satisfies

$$\frac{\partial^2 f_1}{\partial n^2} + \alpha_1 \frac{\partial f_1}{\partial n} + \alpha_2 f_1 = n g_H \quad , \tag{3.19}$$

where

$$f_1(0) = 0, \tag{3.20}$$

$$\left(\frac{\partial f_1}{\partial n}\right)_{n=1} = 0. \tag{3.21}$$

The second particular part is f_2 which satisfies

$$\frac{\partial^2 f_2}{\partial n^2} + \alpha_1 \frac{\partial f_2}{\partial n} + \alpha_2 f_2 = n g_P \quad , \tag{3.22}$$

where

$$f_2(0) = 0, \tag{3.23}$$

$$\left(\frac{\partial f_2}{\partial \eta}\right)_{\eta=1} = 0. \tag{3.24}$$

The boundary condition at the axis is completely satisfied by Equations 3.20 and 3.23. The boundary condition at the wall is

$$f(z,1) = A f_1(z,1) + f_2(z,1) = 1, \tag{3.25}$$

also given by Equation 2.29. This condition is satisfied at each station along the wall by computing the value of A as

$$A(z) = \frac{1 - f_2(z,1)}{f_1(z,1)}. \tag{3.26}$$

Calculation of the constant A allows for complete definition of the total vorticity and the total stream function from Equations 3.10 and 3.18. The stream function is then integrated in the axial direction using the equation

$$\frac{\partial^2 f}{\partial z^2} + \alpha_1 \frac{\partial f}{\partial z} + \alpha_2 f + \alpha_3 - \eta g = 0, \tag{3.27}$$

and the boundary conditions

$$f(0) = A f_1(0) + f_2(0), \tag{3.28}$$

$$\left(\frac{\partial f}{\partial z}\right)_{z=1} = 0. \tag{3.29}$$

The value of A at each station is the boundary condition for the vorticity at the wall as given in Equation 3.17 and also for the stream function as given in Equation 3.25. Thus the boundary condition for vorticity at the wall may be written as

$$g(z,1) = \frac{1 - f_2(z,1)}{f_1(z,1)} = A(z) \; . \qquad 3.30$$

Since a partial derivative with respect to time was included in the stream function, Equation 2.35, it is used as a relaxation parameter. The program iterates on the stream function integrations in both coordinate directions until the f_1 and f_2 matrices converge. During each iteration the value of A(z) is calculated at each station and compared to that of the previous iteration. The iterations halt after A(z) reaches a preset level of accuracy. Upon completion of the iterations, the matrices for the vorticity and the stream functions are valid at the one-half time step.

The vorticity equation is then integrated in the axial direction inputting the matrices from the one-half time step and using the following equation

$$\frac{\partial^2 g}{\partial^2 z} + \alpha_1 \frac{\partial g}{\partial z} + \alpha_2 g + \alpha_3 = 0, \qquad 3.31$$

and the boundary conditions

$$g(0) = \text{any desired input}, \qquad 3.32$$

$$\left(\frac{\partial g}{\partial z}\right)_{z=1} = 0. \qquad 3.33$$

Solution of Equation 3.31 results in a matrix of the vorticity valid at the full time step.

The stream function is then integrated in the normal direction inputting matrices from Equations 3.31 and 3.27 and using the equation

$$\frac{\partial^2 f}{\partial \eta^2} + \alpha_1 \frac{\partial f}{\partial \eta} + \alpha_2 f + \alpha_3 - \eta g = 0, \qquad 3.34$$

and the boundary conditions

$$f(0) = 0, \qquad 3.35$$

$$\left(\frac{\partial f}{\partial \eta}\right)_{\eta=1} = 0. \qquad 3.36$$

The numerical solutions to Equations 3.31 and 3.34 are then used as the input for the integration of the stream function in the axial direction. The equation and boundary conditions used in the axial integration are

$$\frac{\partial^2 f}{\partial z^2} + \alpha_1 \frac{\partial f}{\partial z} + \alpha_2 f + \alpha_3 - \eta g = 0, \qquad 3.37$$

and the boundary conditions

$$f(0) = \text{any desired input}, \qquad 3.38$$

$$\left(\frac{\partial f}{\partial z}\right)_{z=1} = 0. \qquad 3.39$$

Since the updated vorticity matrix is used as an input in solving Equation 3.34 and 3.37, the stream function is also updated by iteration on the integrations in both coordinate directions until convergence is reached. Upon completion of this loop the matrices for vorticity and the stream function are valid at the full time step. The program increments time and the process is repeated for a finite number of time steps until the vorticity matrix converges to the exact solution at a preset level of accuracy.

IV. RESULTS AND CONCLUSIONS

The main result of this study is a blood flow model based on the two-dimensional, nonlinear, unsteady Navier-Stokes equations. The model allows for variations in wave speed, changes in vessel diameter and local outflow. A simplified version of this general model is used to test the numerical scheme, since the general equations contain secondary conditions only in the nonlinear coefficients.

Numerical results obtained from this study stem from two sources: a) test case programs of only the stream function equation or vorticity equation and b) a combined program in which both the stream function and vorticity are integrated. The first category of results are cases in which the initial conditions for the stream function and vorticity are zero and Poiseuille flow is imposed at the proximal end of the vessel.

Figure 6 illustrates results from the vorticity test program with zero initial conditions using nondimensional time steps of 0.16 and a Reynolds number of 100. In solving the vorticity equation, the matrix illustrates a tendency to oscillate about the correct solution. In this steady state case, a simple arithmetic average of the matrix at the previous time step with the matrix at the forward time step allows quick convergence by smoothing out the oscillations. The solution converges rapidly near the axis with the rate of convergence decreasing as it approaches the vessel wall. The graphs of the three selected points in the matrix converge to the exact solution.

Figure 7 illustrates results from the stream function test program with zero initial conditions using nondimensional time steps of

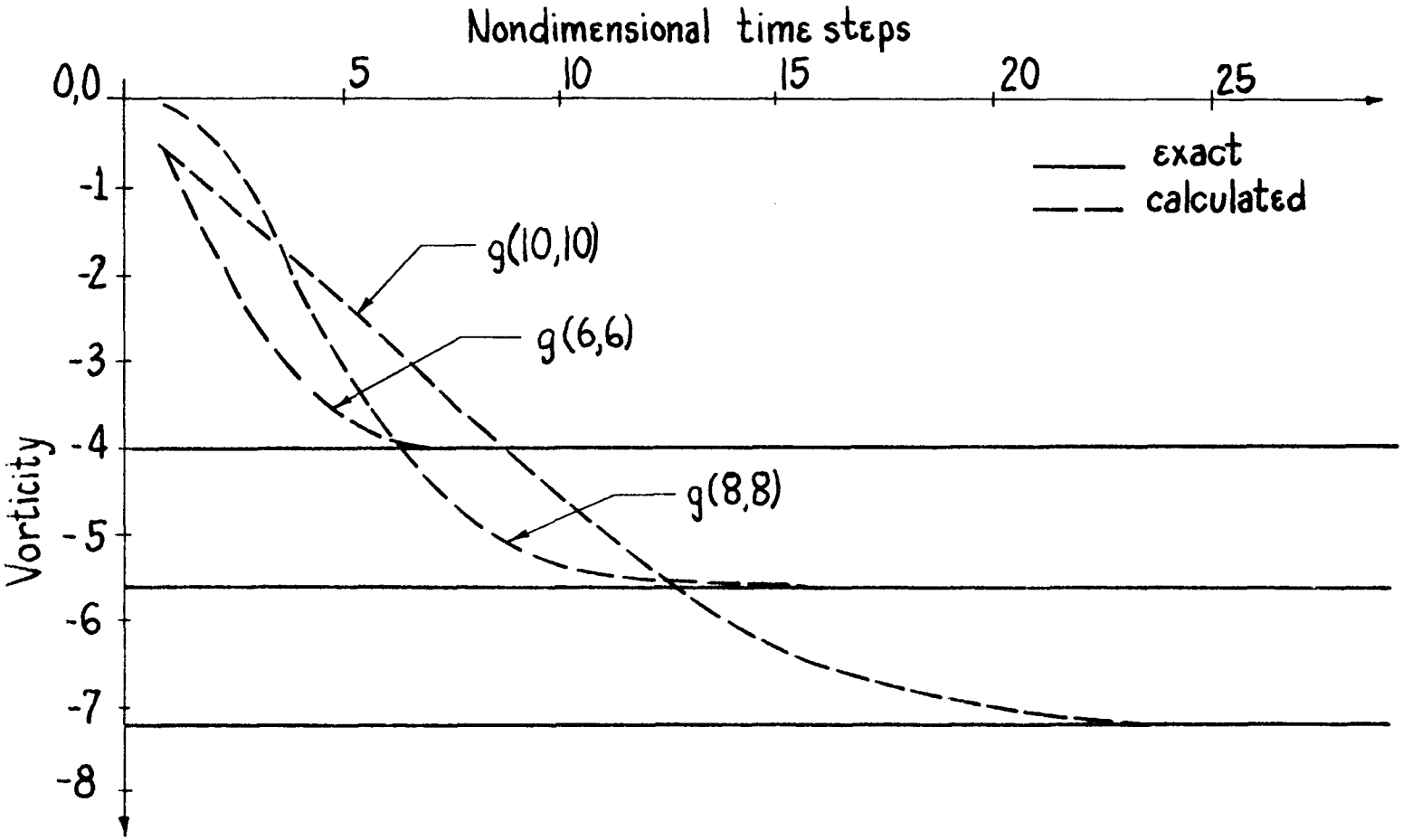

Figure 6. Vorticity test case, zero initial conditions

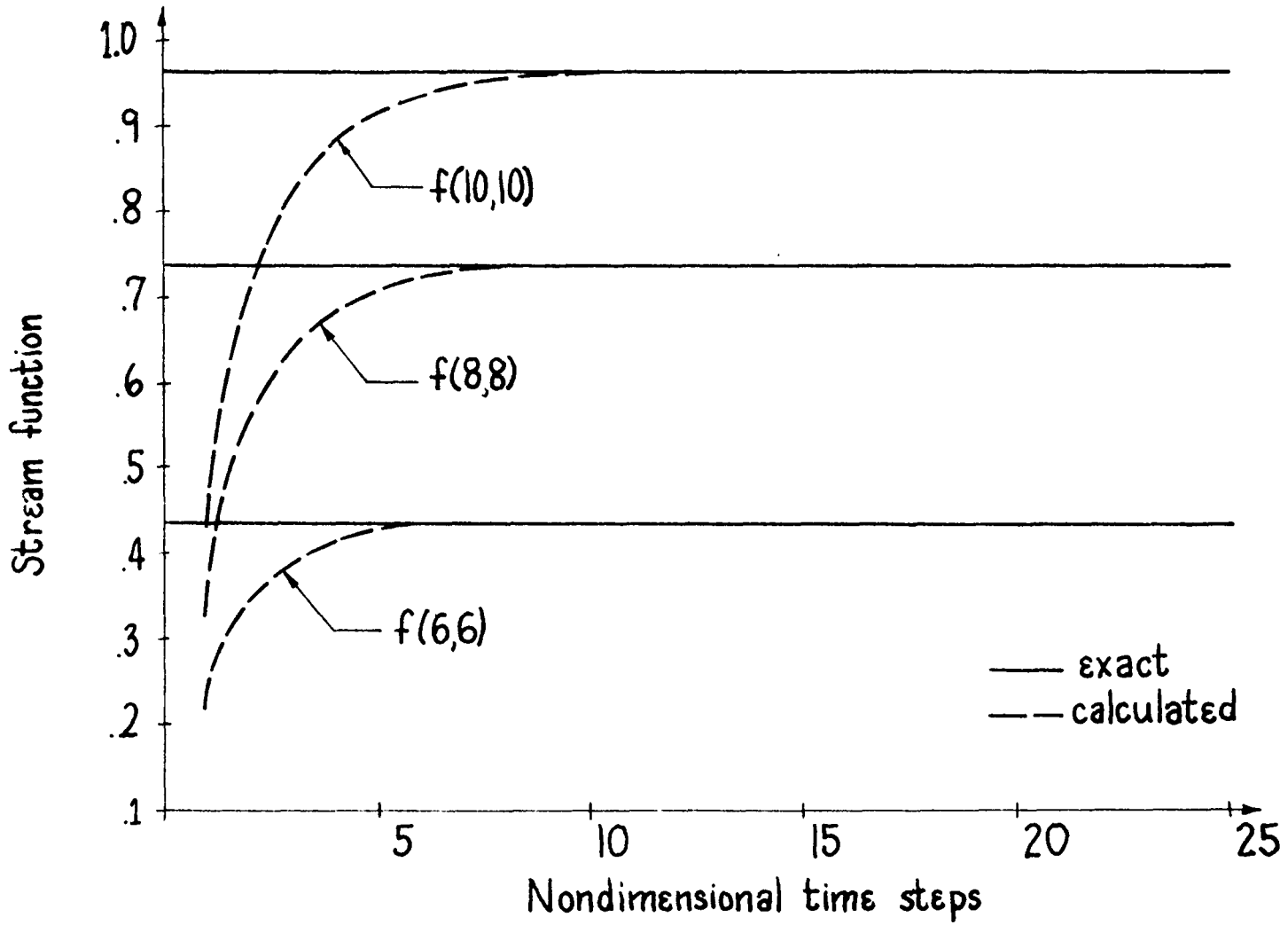

Figure 7. Stream function test case, zero initial conditions

0.16 and a Reynolds number of 100. Again the solution converges very rapidly near the axis with the rate of convergence decreasing as it approaches the wall. Graphs of the three selected points converge to within 2.4 percent of the exact solution.

Figures 8 and 9 illustrate results from the combined program with both the stream function and the vorticity initialized to zero. Poiseuille flow is imposed at the proximal end of the vessel with nondimensional time steps of 0.16 and a Reynolds number of 100. The vorticity matrix is averaged as described previously. The values of A(z) exhibit oscillations due to changes in the f_2 matrix. A simple arithmetic average of the f_2 matrix at the previous and forward iteration steps removes the oscillations in A(z) and allows quicker convergence. Figure 8 shows that the vorticity converges to the exact solution very quickly at points near the axis similar to results of the test case. The solution near the wall converges less rapidly to within five percent accuracy. Figure 9 shows the stream function for the first loop of iterations during the first time step. Iterations at subsequent time steps exhibit even faster convergence. The three selected points in the matrix converge to within one percent of the exact solution.

The second category of results is from cases in which the initial conditions are chosen identical to the anticipated steady state solution. Pulsating Poiseuille flow is introduced into the nonlinear coefficients of the vorticity equation with nondimensional time steps of 0.01, a Reynolds number of 100, and the product of frequency and time equal to 0.16. Figure 10 illustrates the vorticity during the

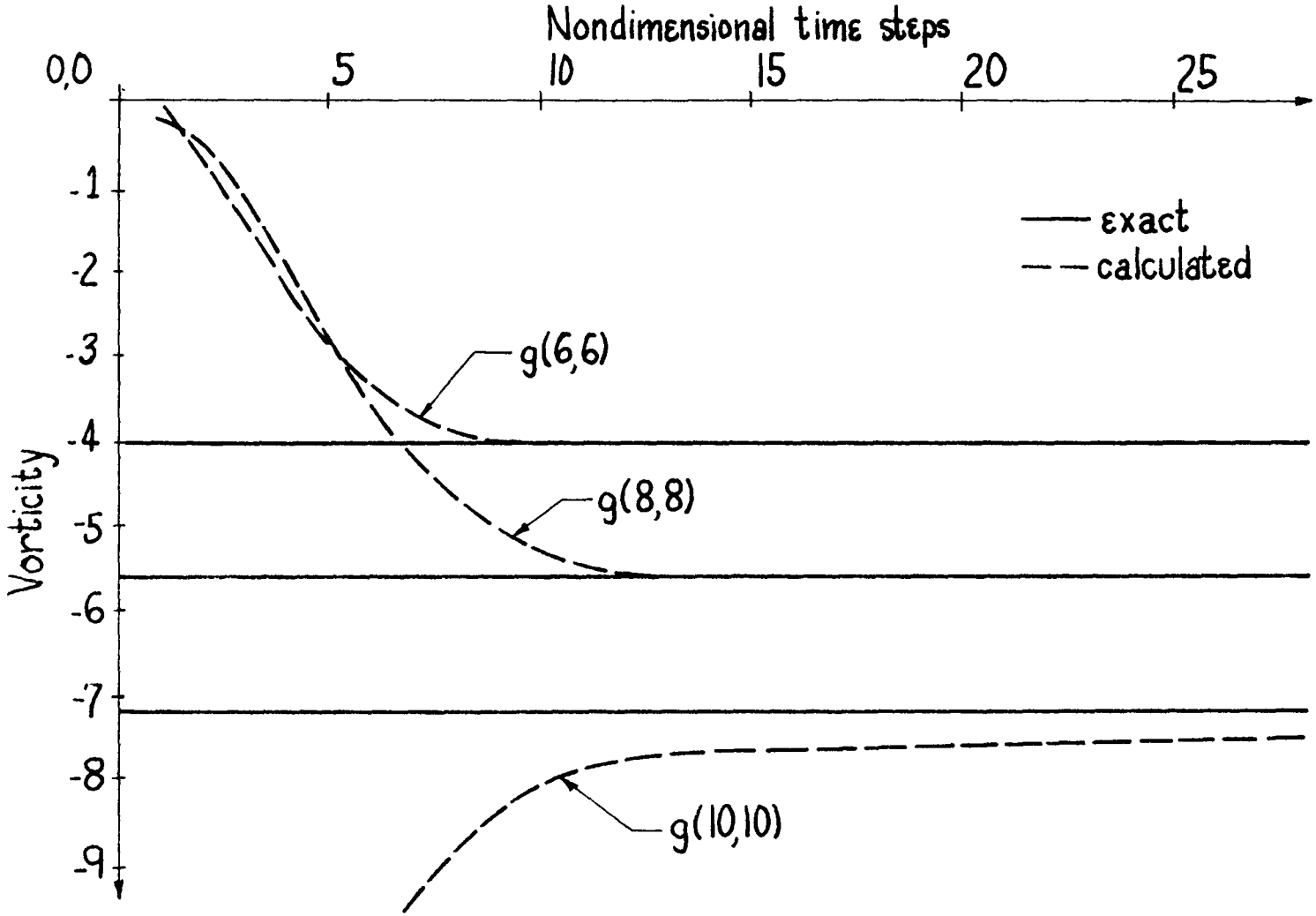

Figure 8. Vorticity in combined program, zero initial conditions

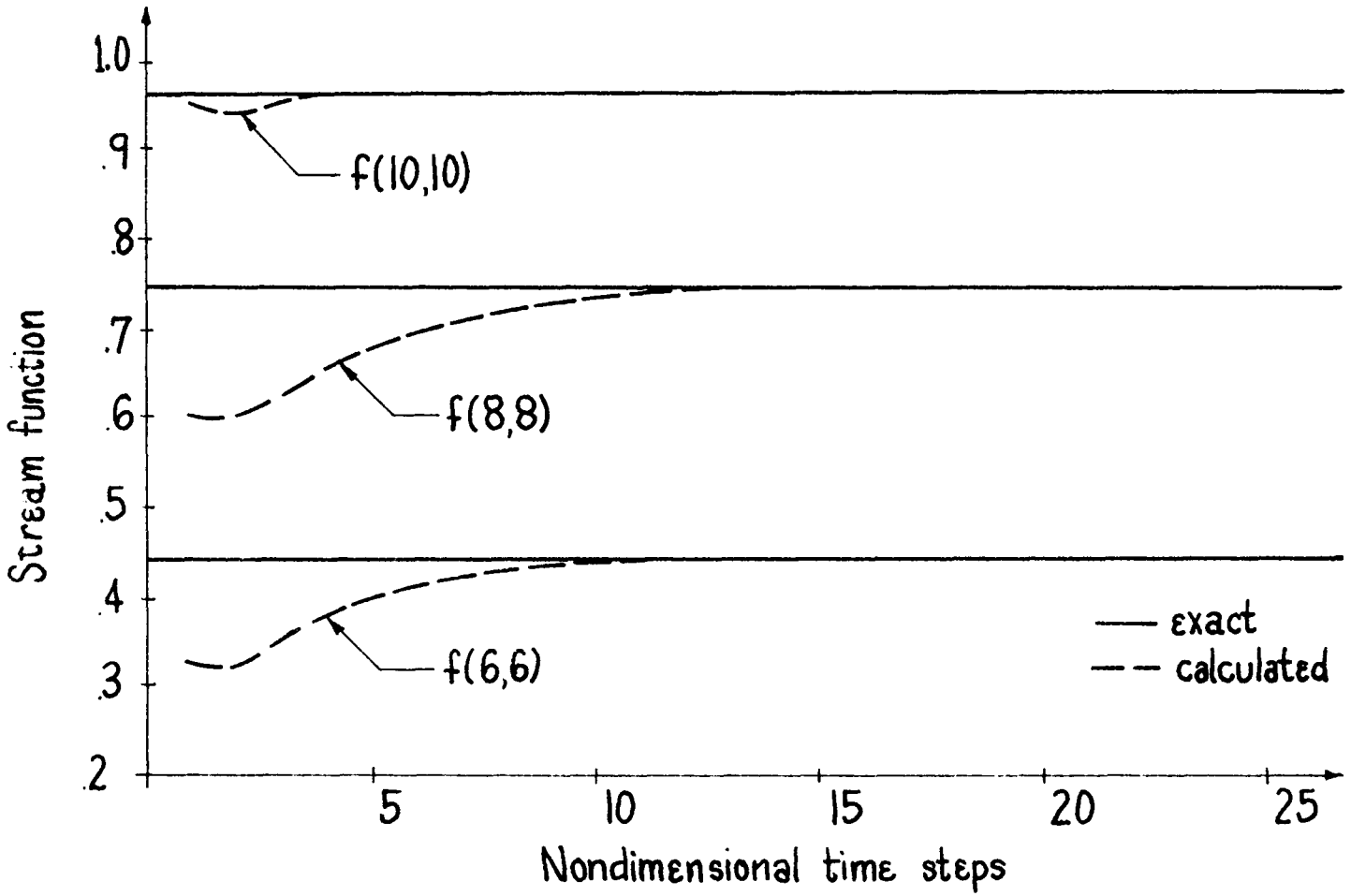

Figure 9. Stream function in combined program, zero initial conditions

first quarter period. The effect of the pulsating input is seen by comparison with the exact steady state solution. The vorticity matrix exhibits oscillations as noted previously, but an arithmetic average over time is not justifiable for the unsteady case. Therefore, large oscillations in the solution occur at and near the vessel wall. Figure 11 illustrates the stream function during the first quarter period. The stream function matrix exhibits oscillations about the exact steady state solution.

In conclusion, the following recommendations are made concerning further extension of this study: a) modifications in the numerical scheme must be made in order to eliminate the oscillations that appear in both the steady state and pulsating cases, b) the computer program should be modified to accommodate backflow in order that a full period of oscillation can be computed, c) the program could be modified to accommodate flow profiles other than Poiseuille.

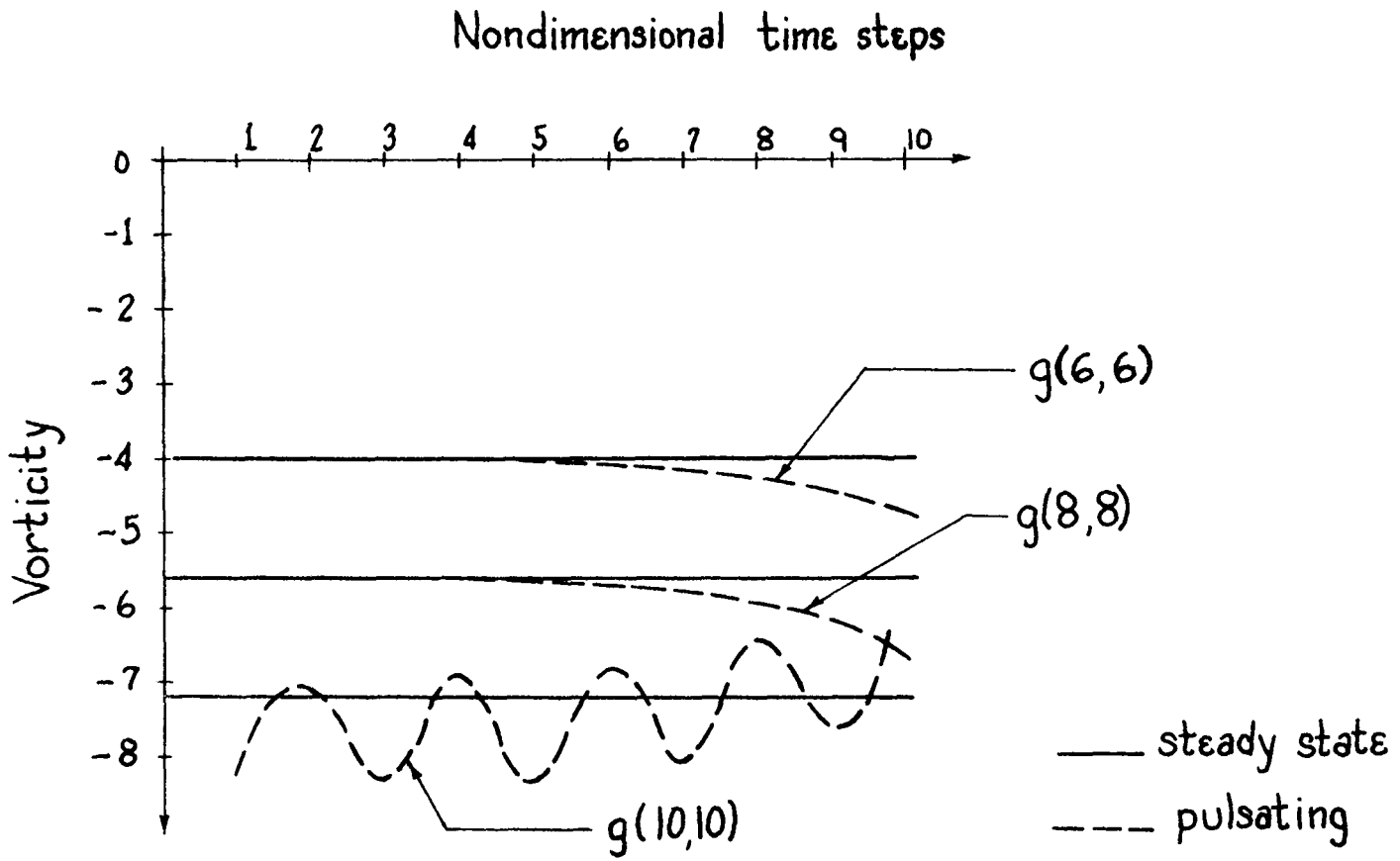

Figure 10. Vorticity in combined program, pulsating case

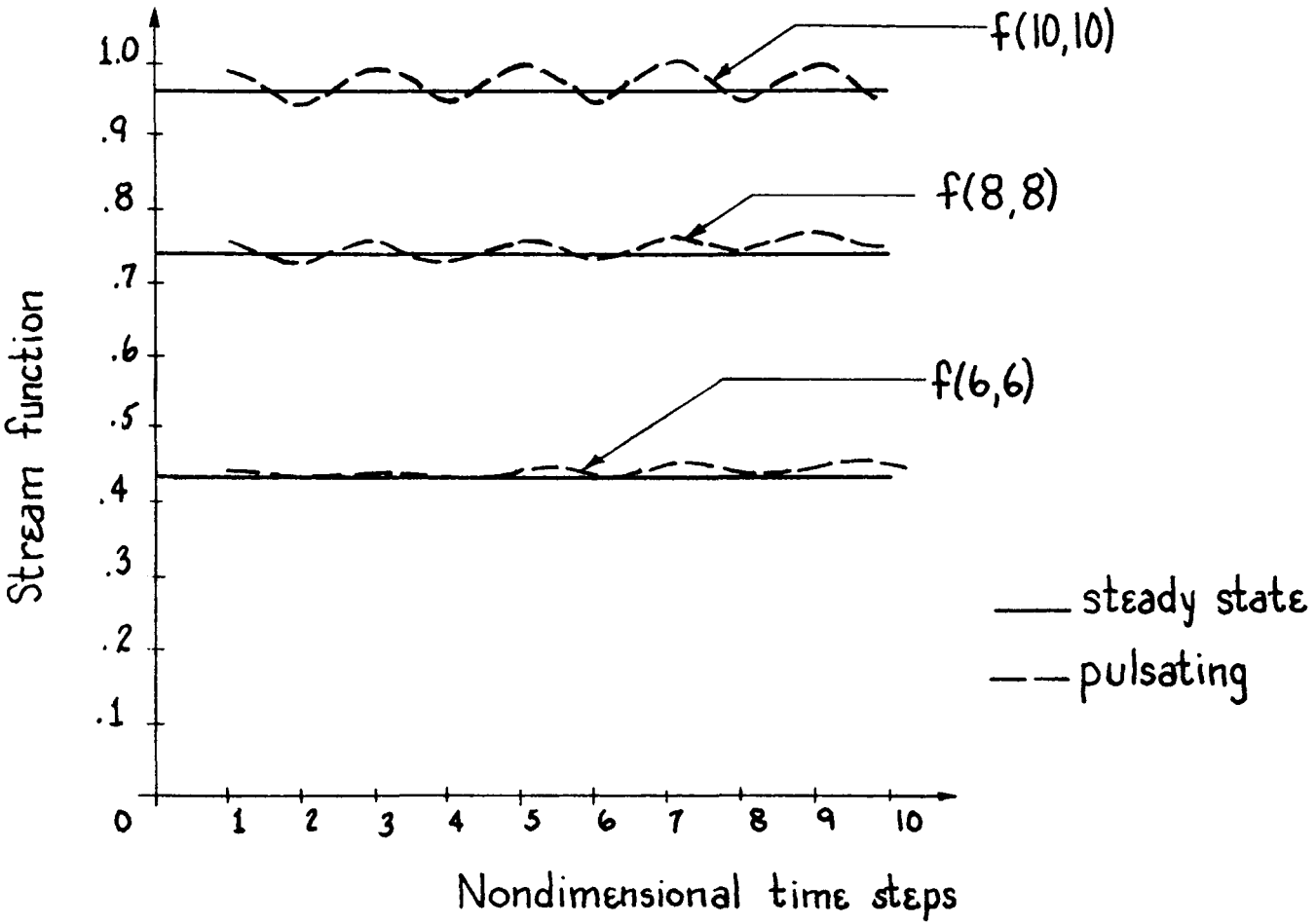

Figure 11. Stream function in combined program, pulsating case

BIBLIOGRAPHY

1. Leake, Chauncey D., "The Historical Development of Cardiovascular Physiology," Section 2, Circulation, Volume I: Handbook of Physiology. Washington, D. C.: American Physiological Society, 1962.

2. Anliker, Max; Rockwell, Robert L,; and Ogden, Eric, "Theoretical Analysis of Nonlinear Phenomena Affecting the Pressure and Flow Pulse in Arteries," Advisory Group for Aerospace Research and Development Conference Proceedings on the Fluid Dynamics of Blood Circulation and Respiratory Flow No. 65. London: Harford House, 1970.

3. Rudinger, George, "Review of Current Mathematical Models for the Analysis of Blood Flow," Biomedical Fluid Mechanics Symposium. New York: American Society of Mechanical Engineers, 1966.

4. Attinger, E. O., "Hydrodynamics of Blood Flow," Advances in Hydroscience; Edited by Ven Te Chou. New York: Academic Press, 1966.

5. Vander, Arthur J.; Sherman, James H.; and Luciano, Dorothy S., Human Physiology: The Mechanisms of Body Function. New York: McGraw Hill Book Company, 1970.

6. Whitmore, R. L., Rheology of the Circulation. Oxford: Pergamon Press, 1968.

7. Elliot, Alfred M., and Ray, Charles Jr., Biology. New York: Meredith Publishing Company, 1965.

8. Burton, A. C., Physiology and Biophysics of the Circulation. Chicago: Year Book Medical Publishers, 1965.

9. Carnahan, Brice; Luther, H. A.; and Wilkes, J. O., Applied Numerical Methods. New York: Wiley and Sons, Inc., 1969.

VI. APPENDIX

THE COMPUTER PROGRAM

```
      IMPLICIT REAL*8 (A-H, O-Z)
      DIMENSION W(11),G(11,11),GHS(11,11),GPS(11,11),GOLD(11,11),
     1F(11,11),F1(11,11),F2(11,11),FS(11,11),ANEW(11),GS(11,11),
     2F2OLD(11,11)
      COMMON/PEQS/A1(11),A2(11),A3(11)
C
C ***** BOOK KEEPING *****
C
      READ(5,110) DTAU,DTAF,RE,IEND,JEND
  110 FORMAT(3F10.4,5X,2I4)
      DTIME=DTAU/2.DO
      DTIMF=DTAF/2.DO
      GRIDX=IEND-1
      DELX=1.0DO/GRIDX
      GRIDY=JEND-1
      DELY=1.0DO/GRIDY
      K=JEND-1
      K2=JEND-2
      L=IEND-1
      L2=IEND-2
      TIME = 0.0DO
      OMEGAT=0.DO
      DOMGAT=0.16DO
      WRITE(6,119)
  119 FORMAT(/8X,4HDTAU,4X,4HDTAF,4X,2HRE,6X,4HDELX,4X,4HDELY,4X,4HIEND,
     12X,4HJEND,2X,6HDOMGAT)
      WRITE(6,120) DTAU,DTAF,RE,DELX,DELY,IEND,JEND,DOMGAT
  120 FORMAT(5X,5F8.3,2X,I4,2X,I4,F8.2/)
C
C***** INITIALIZE THE F AND G MATRICES *****
C
      DO 129 J=1,JEND
```

```
      DO 129 I=1,IEND
      YJ=J-1
      G(I,J)=-8.D0*YJ*DELY
      F(I,J)=(2.D0*((YJ*DELY)**2))-((YJ*DELY)**4)
      F2(I,J)=F(I,J)
      F2OLD(I,J)=F(I,J)
  129 CONTINUE
C
C***** INTEGRATE G IN THE N DIRECTION TO GET GHS(I,J) AND GPS(I,J) *****
C
      GOLDC=-7.2D0
  133 DO 1 I=1,IEND
      DO 1 J=1,JEND
    1 GOLD(I,J)=G(I,J)
      AOLD=0.D0
      DO 132 I=2,L
      DO 141 J=2,K
      YJ=J-1
      W(J)=G(I,J)
      A1(J)=(1.D0/(YJ*DELY))+((RE/(YJ*DELY))*((F(I+1,J)-F(I-1,J))/
     1(2.D0*DELX)))*DCOS(OMEGAT)
      A2(J)=-((1.D0/((YJ*DELY)**2))+(RE/DTIME)+((RE/((YJ*DELY)**2))*
     1((F(I+1,J)-F(I-1,J))/(2.D0*DELX)))*DCOS(OMEGAT)-(RE*DTAN(OMEGAT)))
  141 A3(J)=0.D0
      D1=0.0D0
      E1=0.0D0
      WEND=1.D0
  131 CALL PEQSO(W,D1,E1,WEND,DELY,DELX,DTIME,K,JEND)
      DO 132 J=1,JEND
      GHS(I,J)=W(J)
  132 CONTINUE
  233 DO 232 I=2,L
```

```
      DO 241 J=2,K
      YJ=J-1
      W(J)=G(I,J)
      A1(J)=(1.D0/(YJ*DELY))+((RE/(YJ*DELY))*((F(I+1,J)-F(I-1,J))/
     1(2.D0*DELX)))*DCOS(OMEGAT)
      A2(J)=-((1.D0/((YJ*DELY)**2))+(RE/DTIME)+((RE/((YJ*DELY)**2))*
     1((F(I+1,J)-F(I-1,J))/(2.D0*DELX)))*DCOS(OMEGAT)-(RE*DTAN(OMEGAT)))
  241 A3(J)=((G(I+1,J)-2.D0*G(I,J)+G(I-1,J))/(DELX*DELX))-((RE/(YJ*
     1DELY))*((F(I,J+1)-F(I,J-1))/(2.D0*DELY))*((G(I+1,J)-G(I-1,J))/
     2(2.D0*DELX)))*DCOS(OMEGAT)+(RE*W(J)/DTIME)
      D1=0.0D0
      E1=0.0D0
      WEND=0.D0
  231 CALL PEQSC(W,D1,E1,WEND,DELY,DELX,DTIME,K,JEND)
      DO 232 J=1,JEND
      GPS(I,J)=W(J)
  232 CONTINUE
C
C***** INTEGRATE F IN THE N DIRECTION TO GET F1(I,J) AND F2(I,J) *****
C
      ITNO=0
   33 DO 32 I=2,L
      DO 41 J=2,K
      M=JEND-J+1
      YJ=M-1
      W(J)=F(I,M)
      A1(J)=+1.D0/(YJ*DELY)
      A2(J)=-1.0D0/DTIMF
   41 A3(J)=-((YJ*DELY)*GHS(I,M))
      A=((A1(2)*DTIMF)/(2.0D0*DELY))-(DTIMF/(DELY*DELY))
      B=((2.D0*DTIMF)/(DELY*DELY))-(A2(2)*DTIMF)
      C=-((DTIMF/(DELY*DELY))+((A1(2)*DTIMF)/(2.D0*DELY)))
```

```
      CD=(A3(2))*DTIMF
      DERIV=0.DO
      D1=(B+4.DO*C)/(3.DO*C-A)
      E1=(CD+2.DO*DELY*C*DERIV)/(A-3.DO*C)
      WEND=0.0DO
   31 CALL PEQSO(W,D1,E1,WEND,DELY,DELX,DTIMF,K,JEND)
      DO 32 J=1,JEND
      M=JEND-J+1
      F1(I,J)=W(M)
   32 CONTINUE
  333 DO 16 I=1,IEND
      DO 16 J=1,JEND
   16 F2OLD(I,J)=F2(I,J)
      DO 332 I=2,L
      DO 341 J=2,K
      M=JEND-J+1
      YJ=M-1
      W(J)=F(I,M)
      A1(J)=+1.DO/(YJ*DELY)
      A2(J)=-1.CDO/DTIMF
  341 A3(J)=(W(J)/DTIMF)+((F(I-1,M)-2.DO*F(I,M)+F(I+1,M))/(DELX*DELX))
     1-((YJ*DELY)*GPS(I,M))
      A=((A1(2)*DTIMF)/(2.0DO*DELY))-(DTIMF/(DELY*DELY))
      B=((2.DO*DTIMF)/(DELY*DELY))-(A2(2)*DTIMF)
      C=-((DTIMF/(DELY*DELY))+((A1(2)*DTIMF)/(2.DO*DELY)))
      CD=(A3(2))*DTIMF
      DERIV=0.DO
      D1=(B+4.DO*C)/(3.DO*C-A)
      E1=(CD+2.DO*DELY*C*DERIV)/(A-3.DO*C)
      WEND=0.0DO
  331 CALL PEQSO(W,D1,E1,WEND,DELY,DELX,DTIMF,K,JEND)
      DO 332 J=1,JEND
```

```
      M=JEND-J+1
      F2(I,J)=0.5D0*W(M) + 0.5D0*F2OLD(I,J)
  332 CONTINUE
C
C***** EVALUATE A *****
C
      DO 335 I=2,L
  335 ANEW(I)=(1.D0-F2(I,JEND))/F1(I,JEND)
      ANEWC=ANEW(10)
C
C***** ADD MATRICES TO DEFINE FUNCTIONS FS AND GS COMPLETELY *****
C
      DO 500 I=2,L
      DO 500 J=1,JEND
      FS(I,J)=(ANEW(I)*F1(I,J))+F2(I,J)
      GS(I,J)=(ANEW(I)*GHS(I,J))+GPS(I,J)
  500 CONTINUE
      DO 501 J=1,JEND
      FS(1,J)=F(1,J)
      FS(IEND,J)=(4.D0*FS(L,J)-FS(L2,J))/3.D0
      GS(1,J)=G(1,J)
      GS(IEND,J)=(4.D0*GS(L,J)-GS(L2,J))/3.D0
  501 CONTINUE
C
C***** INTEGRATE F IN THE Z DIRECTION TO GET F(I,J) *****
C
   53 DO 52 J=2,K
      DO 61 I=2,L
      YJ=J-1
      N=IEND-I+1
      W(I)=FS(N,J)
      A1(I)=0.0D0
```

```
      A2(I)=-1.0D0/DTIMF
   61 A3(I)=W(I)/DTIMF+(FS(N,J-1)-2.D0*FS(N,J)+FS(N,J+1))/(DELY*DELY)
     1-(FS(N,J+1)-FS(N,J-1))/(YJ*DELY*DELY*2.D0)-((YJ*DELY)*GS(N,J))
      A=((A1(2)*DTIMF)/(2.0D0*DELX))-(DTIMF/(DELX*DELX))
      B=(2.D0*DTIMF/(DELX*DELX))-(A2(2)*DTIMF)
      C=-((DTIMF/(DELX*DELX))+((A1(2)*DTIMF)/(2.D0*DELX)))
      CD=A3(2)*DTIMF
      DERIV=0.D0
      D1=(B+4.DC*C)/(3.D0*C-A)
      E1=(CD+2.D0*DELX*C*DERIV)/(A-3.D0*C)
      WEND=((2.D0*((YJ*DELY)**2))-((YJ*DELY)**4))
   51 CALL PEQSO(W,D1,E1,WEND,DELX,DELY,DTIMF,L,IEND)
      DO 52 I=1,IEND
      N=IEND-I+1
      F(I,J)=W(N)
   52 CONTINUE
      DO 55 I=2,IEND
      F(I,1)=FS(I,1)
      F(I,JEND)=FS(I,JEND)
   55 CONTINUE
C
C***** CHECK CONVERGENCE AT THE HALF TIME STEP *****
C
      ANEWB=DABS(ANEWC)
      IF(ANEWB.LE.0.01D0) GO TO 79
      CNVG1=DABS((ANEWC-AOLD)/ANEWC)
      AOLD=ANEWC
      ITNO=ITNO+1
      IF(CNVG1-0.01D0)821,821,333
   79 AOLD=ANEWC
      ITNO=ITNO+1
  821 ITNO=0
```

```
      TIME=TIME+DTIME
      WRITE(6,337) (ANEW(I),I=2,L)
  337 FORMAT(/1X,7HANEW IS,5X,9D11.3/)
      WRITE(6,813) CNVG1
  813 FORMAT(5X,8HCNVG1 = ,D11.3)
C
C***** INTEGRATE G IN THE Z DIRECTION *****
C
  453 DO 452 J=2,K
      YJ=J-1
      DO 461 I=2,L
      N=IEND-I+1
      W(I)=GS(N,J)
      A1(I)=+((RE/(YJ*DELY))*((F(N,J+1)-F(N,J-1))/(2.D0*DELY)))*
     1DCOS(OMEGAT)
      A2(I)=-((1.D0/((YJ*DELY)**2))+(RE  /DTIME)-((RE/((YJ*DELY)**2))*
     1((F(N+1,J)-F(N-1,J))/(2.D0*DELX)))*DCOS(OMEGAT)-(RE*DTAN(OMEGAT)))
  461 A3(I)=((GS(N,J+1)-2.D0*GS(N,J)+GS(N,J-1))/(DELY*DELY))+
     1(RE*W(I)/DTIME)+((1.D0/(YJ*DELY))-((RE/(YJ*DELY))*((F(N+1,J)-
     2F(N-1,J))/(2.D0*DELX)))*DCOS(OMEGAT))*((GS(N,J+1)-GS(N,J-1))
     3/(2.D0*DELY))
      A=((A1(2)*DTIME)/(2.0D0*DELX))-(DTIME/(DELX*DELX))
      B=((2.D0*DTIME)/(DELX*DELX))-(A2(2)*DTIME)
      C=-((DTIME/(DELX*DELX))+((A1(2)*DTIME)/(2.D0*DELX)))
      CD=(A3(2))*DTIME
      DERIV=0.D0
      D1=(B+4.D0*C)/(3.D0*C-A)
      E1=(CD+2.D0*DELX*C*DERIV)/(A-3.D0*C)
      WEND=-8.D0*YJ*DELY
  451 CALL PEQSO(W,D1,E1,WEND,DELX,DELY,DTIME,L,IEND)
      DO 452 I=1,IEND
      N=IEND-I+1
```

```
      G(I,J)=W(N)
  452 CONTINUE
      DO 460 I=1,IEND
      G(I,1)=0.0D0
      G(I,JEND)=2.D0*G(I,K)-G(I,K2)
  460 CONTINUE
      TIME=TIME+DTIME
      DMULT=DCOS(OMEGAT)
      OMEGAT=OMEGAT+DOMGAT
      WRITE(6,681) TIME,DMULT
  681 FORMAT(//5X,7HTIME = ,F8.5,5X,8HDMULT = ,D11.3/)
      WRITE(6,814)
  814 FORMAT(2X,47HTHIS IS THE G(I,J) MATRIX AT THE FULL TIME STEP/)
      WRITE(6,815) ((G(I,J),I=1,IEND),J=1,JEND)
  815 FORMAT(2X,11D11.3)
C
C ***** INTEGRATE F IN N DIRECTION *****
C
      ITNO=0
      FOLD=0.D0
  633 DO 600 I=2,L
      DO 641 J=2,K
      M=JEND-J+1
      W(J)=F(I,M)
      YJ=M-1
      A1(J)=+1.D0/(YJ*DELY)
      A2(J)=-1.0D0/DTIMF
  641 A3(J)=(W(J)/DTIMF)+((F(I-1,M)-2.D0*F(I,M)+F(I+1,M))/(DELX*DELX))
     1-((YJ*DELY)*G (I,M))
      A=((A1(2)*DTIMF)/(2.0D0*DELY))-(DTIMF/(DELY*DELY))
      B=(2.D0*DTIMF/(DELY*DELY))-(A2(2)*DTIMF)
      C=-((DTIMF/(DELY*DELY))+((A1(2)*DTIMF)/(2.D0*DELY)))
```

```
      CD=(A3(2))*DTIMF
      DERIV=C.DO
      D1=(B+4.DO*C)/(3.DO*C-A)
      E1=(CD+2.DO*DELY*C*DERIV)/(A-3.DO*C)
      WEND=0.0DO
      CALL PEQSO(W,D1,E1,WEND,DELY,DELX,DTIMF,K,JEND)
      DO 600 J=1,JEND
      M=JEND-J+1
      FS(I,J)=W(M)
  600 CONTINUE
      DO 601 J=1,JEND
      FS(1,J)=F(1,J)
      FS(IEND,J)=(4.DO*FS(L,J)-FS(L2,J))/3.DO
  601 CONTINUE
C
C***** INTEGRATE FS IN THE Z DIRECTION  *****
C
      DO 752 J=2,K
      DO 761 I=1,IEND
      YJ=J-1
      N=IEND-I+1
      W(I)=FS(N,J)
      A1(I)=0.0DO
      A2(I)=-1.0DO/DTIMF
  761 A3(I)=W(I)/DTIMF+(FS(N,J-1)-2.DO*FS(N,J)+FS(N,J+1))/(DELY*DELY)
     1-(FS(N,J+1)-FS(N,J-1))/(YJ*DELY*DELY*2.DO)-((YJ*DELY)*G(N,J))
      A=((A1(2)*DTIMF)/(2.0DO*DELX))-(DTIMF/(DELX*DELX))
      B=(2.DO*DTIMF/(DELX*DELX))-(A2(2)*DTIMF)
      C=-((DTIMF/(DELX*DELX))+((A1(2)*DTIMF)/(2.DO*DELX)))
      CD=A3(2)*DTIMF
      DERIV=0.DO
      D1=(B+4.DO*C)/(3.DO*C-A)
```

```
      E1=(CD+2.D0*DELX*C*DERIV)/(A-3.D0*C)
      WEND=FS(1,J)
      CALL PEQSO(W,D1,E1,WEND,DELX,DELY,DTIMF,L,IEND)
      DO 752 I=1,IEND
      N=IEND-I+1
      F(I,J)=W(N)
  752 CONTINUE
C
C ***** CHECK CONVERGENCE AT THE FULL TIME STEP *****
C
      ITNO=ITNO+1
      FNEW=F(10,10)
      CNVF=DABS((FNEW-FOLD)/FNEW)
      FOLD=FNEW
      WRITE(6,13) CNVF,ITNO
   13 FORMAT(/5X,7HCNVF = ,D11.3,8X,19HITERATION NUMBER = ,I4)
      IF(CNVF.GE.0.01D0) GO TO 633
      WRITE(6,683)
  683 FORMAT(1X,47HTHIS IS THE F(I,J) MATRIX AT THE FULL TIME STEP/)
      WRITE(6,684) ((F(I,J),I=1,IEND),J=1,JEND)
  684 FORMAT(2X,11D11.3)
      GNEW=G(10,10)
      CNVGV=DABS((GNEW-GOLDC)/GNEW)
      GOLDC=-7.2D0
      WRITE(6,14) CNVGV
   14 FORMAT(/5X,8HCNVGV = ,D11.3)
      IF(OMEGAT.LE.6.28D0) GO TO 133
      STOP
      END
```

```
      SUBROUTINE PEQSO(W,D1,E1,WEND,DELN,DELZ,DTIME,KL,IJEND)
      IMPLICIT REAL*8 (A-H, O-Z)
      DIMENSION W(11),D(11),E(11)
      COMMON/PEQS/A1(11),A2(11),A3(11)
      AMBDA = DTIME/(DELN*DELN)
      D(1)=D1
      E(1)=E1
      W(KL+1)=WEND
      DO 40 I=2,KL
      A=((A1(I)*DTIME)/(2.0D0*DELN))-AMBDA
      B=(2.0D0*AMBDA)-(A2(I)*DTIME)
      C=-(AMBDA+((A1(I)*DTIME)/(2.D0*DELN)))
      CD=A3(I)*DTIME
      D(I)=-C/(A*D(I-1)+B)
   40 E(I)=(CD-A*E(I-1))/(A*D(I-1)+B)
      DO 50 I=1,KL
      N=IJEND-I
   50 W(N) = D(N)*W(N+1) + E(N)
      RETURN
      END
```

The vita has been removed from the scanned document

PULSATILE BLOOD FLOW IN THE ARTERIES

by

Gloria Adame Bennett

(ABSTRACT)

The present study develops the unsteady, nonlinear, two-dimensional partial differential equations for pulsatile flow in a flexible tube. The fluid is assumed to be a Newtonian, incompressible liquid similar to blood. The vessel is modeled as circular in cross section and tapering with increasing distance from the heart. The governing equations are solved numerically using a finite difference form of the Navier-Stokes equations and the Alternating Direction Implicit method. The purpose of this study is to solve a simplified version of the general equations in order to demonstrate the feasibility of solving this type of system numerically.